Supplemental Materials and Methods

Chemicals, dyes, Antibodies, and recombinant proteins:

IBMX, dexamethasone, indomethacin and recombinant human insulin were purchased from Sigma-Aldrich (Burlington, MA, USA). BODIPY 493/503 (lipid dye) was purchased from Thermo Fisher Scientific (Waltham, MA, USA). PHA dye (Rhodamine Phalloidin, actin dye) was purchased from Cytoskeleton (Denver, CO, USA). Zombie Violet (viability dye) was purchased from Biolegend (San Diego, CA, USA). Mouse anti-TPSB2, and goat anti-C/EBPδ antibodies were purchased from Abcam (Cambridge, UK). Goat anti-F3 (CD142) and goat anti-PDGFRA antibodies were purchased from R&D Systems (Minneapolis, MN, USA). Rabbit anti PLIN1, rabbit anti-TPSB2, rabbit anti-pSMAD2/3 and rabbit anti-pSTAT6 antibodies were purchased from Cell Signaling Technology (Danvers, MA, USA). Mouse anti-Vimentin, rabbit anti-KITL, and rabbit anti-CXCL12 were purchased from Proteintech (Rosemont, IL, USA). Recombinant mouse IL4, recombinant mouse IL13, recombinant mouse TGFβ, recombinant mouse IL3, recombinant mouse SCF, recombinant human IL4 and recombinant human IL13 were purchased from R&D Systems (Minneapolis, MN, USA). Recombinant human TGFβ were purchased from PeproTech (Thermo Fisher Scientific, Waltham, MA, USA).

Histology, collagen trichrome staining and immunohistochemistry (IHC):

To prepare paraffin sections, tissue biopsies were fixed in 4% paraformaldehyde (PFA; Alfa Aesar, Shanghai, China) overnight, followed by dehydration, embedding in paraffin, and sectioning at a thickness of 7 μm. For frozen sections, fresh dorsal skin tissues were directly embedded in optimal cutting temperature (OCT) compound and sectioned at 18 μm.

For histological analysis, frozen sections were first fixed in 4% PFA for 15 minutes before staining. Hematoxylin and Eosin (HE) staining (ZSGB-BIO, China) and Masson's Trichrome staining (Solarbio, China) were performed strictly according to the manufacturers' protocols. Lipid staining on frozen sections was conducted using BODIPY (ThermoFisher Scientific, Waltham, MA, USA) and PHA (Cytoskeleton, Denver, CO, USA) dyes.

For immunohistochemistry (IHC), fixed sections were permeabilized with 0.1% saponin (Sigma-Aldrich, St Louis, MO, USA) and blocked in 5% bovine serum albumin (BSA; Bioforxx, Hessen, Germany). The blocked sections were incubated with primary antibodies at 4°C overnight, then with appropriate secondary antibodies conjugated to Alexa Fluor 488, Cy5, or Cy3 (Jackson ImmunoResearch Laboratories, West Grove, PA, USA) for 1.5 hours at room temperature in the dark. Finally, sections were mounted using ProLong Gold Antifade Mountant containing DAPI (Thermo Scientific Inc., Rockford, IL, USA).

All images were acquired using either the Aperio VERSA Brightfield/Fluorescence Digital Pathology Scanner or the Leica TCS SP8 White Light Laser Confocal Microscope, and processed with Adobe Photoshop and/or Aperio ImageScope software (Leica Biosystems, Germany). Quantification of the integrated fluorescence intensity for each fluorophore was performed using ImageJ software.

Flow cytometry and analysis (FACS) and Cell Sorting:

The FACS procedure for analyzing EtOH- or MC903-treated mouse skin dermal fibroblasts and mast cells was modified from previously established or reported method. Briefly, Viable cells were stained with Zombie Violet™ viability dye (BioLegend, 423114) for 15 minutes at room temperature, following by blocking with anti-mouse CD16/32 (1:100; eBioscience, 14-0161-85). Surface staining employed two parallel panels: (1) Fibroblast characterization panel: FITC-conjugated anti-CD26 (BioLegend, 137806), PE-conjugated anti-Thy1.2 (BioLegend, 105308), BV605-conjugated anti-Ly6A/E (BioLegend, 108133), PE-Cy7-conjugated anti-CD45 (BioLegend, 103114), APC-conjugated anti-PDGFRα (BioLegend, 135910), and PE-conjugated anti-F3 (R&D Systems, FAB3178P). (2) Mast cell profiling panel: PE-Cy7-conjugated anti-CD45 (BioLegend, 103114), PE-conjugated anti-FcεR1α (BioLegend, 134307), and APC-conjugated anti-c-Kit (BioLegend, 135108).

FACS analysis of protein expression for each cell marker was conducted using a Cytoflex LX flow cytometer, with data analyzed via FlowJo V10 software.

For FACS sorting of inflammatory preadipocytes from MC903-treated mouse skin, a Cytoflex SRT machine was used. Immediately after sorting, freshly isolated cells were lysed directly in TRIzol reagent for subsequent qRT-PCR analysis.

Quantitative reverse transcription-quantitative PCR (qRT-PCR) analysis:

Total cellular RNA was extracted using the RNAExpress Total RNA Kit (NCM biotech, Suzhou, China). Reverse transcription of 500 ng RNA to cDNA was performed using the HiScript III RT SuperMix Kit (Vazyme Biotech Co., Ltd., Nanjing, China). Quantitative real-time PCR (qRT-PCR) was conducted on the qTower Real-Time PCR System (Analytik Jena AG, Jena, Germany) using ChamQ Universal SYBR qPCR Master Mix (Vazyme Biotech Co., Ltd., Cat. No. Q711-02).

All primers used with SYBR Green chemistry were designed to span at least one exon-intron junction to avoid nonspecific amplification of genomic DNA. The TATA-box binding protein (*Tbp / TBP*) gene was selected as an internal reference to normalize target gene expression levels in mouse samples. Primer sequences are listed in **Supplementary Table S3 and Table S4**.

ELISA assay

Mouse CXCL12, KITL, IL-4, IL-13, and TGF-β1 ELISA kits were purchased from R&D Systems (Minneapolis, MN, USA). Conditioned media (CM) collected from in vitro differentiated mouse dermal preadipocytes or bone marrow-derived mast cells (BMMCs) were assayed for protein concentrations using these kits following the manufacturer's protocols.

RNA velocity:

To reconstruct the lineage commitment trajectories of dermal fibroblasts (dFBs), we performed RNA velocity analysis using the scVelo package (v0.3.3) with default parameters. Briefly, spliced and unspliced mRNA counts were extracted from aligned

BAM files using the velocyto algorithm (v0.17.17), enabling the prediction of future transcriptional states based on splicing dynamics. Velocity vectors were computed using steady-state modeling to infer directional cell-state transitions, which were subsequently projected onto the UMAP embedding to visualize dFB lineage trajectories.

Gene-set enrichment scores:

We quantified functional signatures across dermal fibroblast (dFB) clusters using Seurat's AddModuleScore function. This method calculates cluster-specific enrichment scores by computing the average expression of signature genes per cell and subtracting background expression from randomly selected control features. Inflammatory signature was formed by: *Il6, Cxcl1*, *Cxcl12*, *Cxcl13*, *Cxcl14*, *Cxcl2*, *Ccl11*, *Ccl2*, *Ccl7*, *Saa3, Kitl, Cebpd, Il33*. Adipocyte signature was formed by: *Pparg*, *Lpl*, *Fabp4*, *Mest*, *Agt*, *Plin1, Plin2*. Preadipocyte signature was formed by: *Kitl*, *Prg4*, *Cxcl12*, *Apoe, Apod, Cebpb, Cebpd*, *Zfp36, F3*. Adipocyte progenitor signature was formed by: *Wnt2, Smpd3, Sfrp2, Anxa3, Col14a1, Pcolce2, Plat, Fn1, Mfap5.* Scores were averaged within all cells from the same cluster and inflammatory or adipogenic region (dFB subsets). This approach enabled systematic comparison of functional states across fibroblast subpopulations.

Pearson Correlation analysis:

To evaluate transcriptional relationships across systems, we performed Pearson correlation analyses on two complementary datasets: 1. In vitro-in vivo comparison: RNA-seq from *in vitro* adipocyte differentiation versus scRNA-seq of dermal fibroblast (dFB) subclusters from MC903-treated mice; 2. Cross-species analysis: scRNA-seq of dFB subclusters from healthy human skin, human atopic dermatitis (AD) lesions, and MC903-treated mouse skin.

For both analyses, raw transcriptomic data were normalized, transformed into expression matrices, and analyzed using Pearson correlation coefficients. Hierarchical clustering results were visualized as heatmaps in R Studio. This integrated approach revealed conserved and divergent signatures between *in vitro* adipogenesis and *in vivo* dFB states, and species-specific and disease-associated dFB subcluster profiles, offering mechanistic insights into skin pathophysiology.

Cell-chat signaling network analysis:

To investigate intercellular communication dynamics among dermal fibroblast (dFB) subclusters and their interactions with immune cells during MC903-induced inflammation, we utilized CellChat (version 2.2.0) for computational analysis of scRNA-seq data. This framework enabled systematic characterization of cell-cell signaling by mapping gene expression profiles onto a ligand-receptor pair network, calculating interaction probabilities to predict biologically relevant communication networks and evaluating network centrality to identify key cell populations in specific signaling pathways. The resulting communication networks were visualized through hierarchical graphs and circle plots, providing a multi-dimensional representation of

both individual and coordinated signaling activities.

Bulk RNA sequencing and bioinformatic analysis:

Total RNA was isolated using TRIzol reagent (Vazyme, R401-01-AA) followed by column purification with the RNAExpress Total RNA Kit (NCM biotech, M050). RNA quality was verified using a Bioanalyzer (Agilent Technologies), with only samples exhibiting RNA Integrity Numbers (RIN) >7 proceeding to library preparation. Libraries were constructed using the NEBNext Ultra RNA Library Prep Kit for Illumina, following the manufacturer's protocol. Briefly:

1. mRNA enrichment: Poly(A)+ RNA was isolated using the NEBNext Poly(A) mRNA Magnetic Isolation Module.
2. cDNA synthesis: Fragmented mRNA underwent first-strand synthesis with ProtoScript II Reverse Transcriptase and random primers, followed by second-strand synthesis using the NEBNext Second Strand Synthesis Enzyme Mix.
3. Library construction: End repair/dA-tailing was performed using the End Prep Enzyme Mix, followed by adapter ligation. Size selection (~420 bp total, ~300 bp insert) was achieved with AxyPrep Mag PCR Clean-up beads (Axygen).
4. Amplification and QC: Libraries were PCR-amplified, purified, and quantified using a Qubit 2.0 Fluorometer (Invitrogen), with size distribution validated on an Agilent 2100 Bioanalyzer.

Multiplexed libraries were sequenced on an Illumina NovaSeq platform (2×150 paired-end). Raw data were processed by GENEWIZ, with downstream analysis including differential gene expression analysis, KEGG and GO pathway enrichment and correlation analysis between single-cell and bulk RNA-seq datasets.

Knockdown experiments by siRNA transfection:

To knockdown *Cxcl12* or *Kitl* expression in differentiating preadipocytes (pAds), the TriFECTa RNAi Kit targeting *Kitl* (Integrated DNA Technologies) and small interfering RNA (siRNA) against *Cxcl12* (JTS Scientific) were used. These RNAi reagents (targeting *Cxcl12* or *Kitl*) were transfected into differentiating pAds using Lipofectamine RNAiMAX (Invitrogen, 13778030). At 48 hours post-dsiRNA transfection, conditioned medium (CM) was collected separately from each treatment group for use in co-culture assays or ELISA analyses. Meanwhile, the differentiating pAds were harvested for qRT-PCR analysis to assess knockdown efficiency.

The sequences targeting *Kitl* were as follows:

si-Kitl#1: sense sequence: 5'-CUA UUCUGUACGCAUUGUUGAAGAA-3′, antisense sequence: 5′-UUCUUCAACAAUGCGUACAGAAUAGCU-3′.

si-Kitl#2: sense sequence: 5'-CAUUGUUGGCUACGAGAUAUGGUAA-3′, antisense sequence: 5′- UUACCAUAUCUCGUAGCCAACAAUGAC-3′.

si-Kitl#3: sense sequence: 5'-GAUAAUGUAAAAGACAUUACAAAAC-3′, antisense sequence: 5′- GUUUUGUAAUGUCUUUUACAUUAUCAG-3′.

The sequences targeting *Cxcl12* were as follows:

si-Cxcl12#1: sense sequence: 5'-GAAGAACAACAACAGACAAGUTT-3′, antisense sequence: 5′- ACUUGUCUGUUGUUGUUCUUCTT-3′.

si-Cxcl12#2: sense sequence: 5'- CUGCAUCAGUGACGGUAAACCTT-3′, antisense sequence: 5′- GGUUUACCGUCACUGAUGCAGTT-3′.
si-Cxcl12#3: sense sequence: 5'- GAUCCAAGAGUACCUGGAGAATT-3′, antisense sequence: 5′- UUCUCCAGGUACUCUUGGAUCTT-3′.

Isolation and In Vitro Culture of Bone Marrow-Derived Mast Cells:

To isolate mast cells, bone marrow cells were first flushed from the femurs and tibias of mice using RPMI-1640 medium supplemented with 10% fetal bovine serum (FBS). The harvested bone marrow cells were treated with red blood cell lysis buffer, followed by a single wash with phosphate-buffered saline (PBS).

For in vitro culture, the isolated cells were maintained in RPMI-1640 medium containing the following supplements:1x antibiotics/antimycotics, 1 mM sodium pyruvate, 1x nonessential amino acids solution, 10% (v/v) FBS, 10 ng/ml recombinant mouse interleukin-3 (IL-3), and 10 ng/ml recombinant mouse stem cell factor (SCF). After 4 weeks of culture, FACS analysis confirmed that >95% of the cells were mast cells (MCs) expressing c-Kit and FcεRIα ($c\text{-}Kit^{+}$ $Fc\varepsilon RI\alpha^{+}$).

Co-Culture of Mast Cells with Conditioned Medium Derived from Inflammatory Preadipocytes:

For direct co-culture experiments, mast cells were treated with a 1:1 mixture of inflammatory preadipocyte-conditioned medium (inf.pAd-CM) and mast cell culture medium for 48 hours. At specified time points, mast cells or their conditioned medium (CM) were harvested for qRT-PCR and ELISA analyses. Supernatants were centrifuged to remove cellular debris, and the resulting clarified fluid was collected as CM.

Quantification and statistical analysis

All experiments were repeated independently at least three times, yielding similar results. Statistical analyses were performed using GraphPad Prism software (version 9.0.0). Immunofluorescence intensity quantification was conducted using ImageJ software (version 1.53). Specifically, integrated density values for each fluorophore were measured within defined regions of interest (ROIs) across epidermal and dermal layers of skin sections. Intensity profiles depicting fluorescence signals along the epidermis-dermis axis (from top to bottom) were generated using established methods adapted from prior publications.

Statistical significance between two experimental conditions was determined using Student's unpaired two-tailed t-test, while one-way analysis of variance (ANOVA) with Tukey's post hoc test was applied for multiple group comparisons. Probability (P) values <0.05 were considered statistically significant, with significance levels denoted as *P<0.05, **P<0.01, ***P<0.001, and ****P<0.0001. Data are presented as mean ± standard error of the mean (SEM).

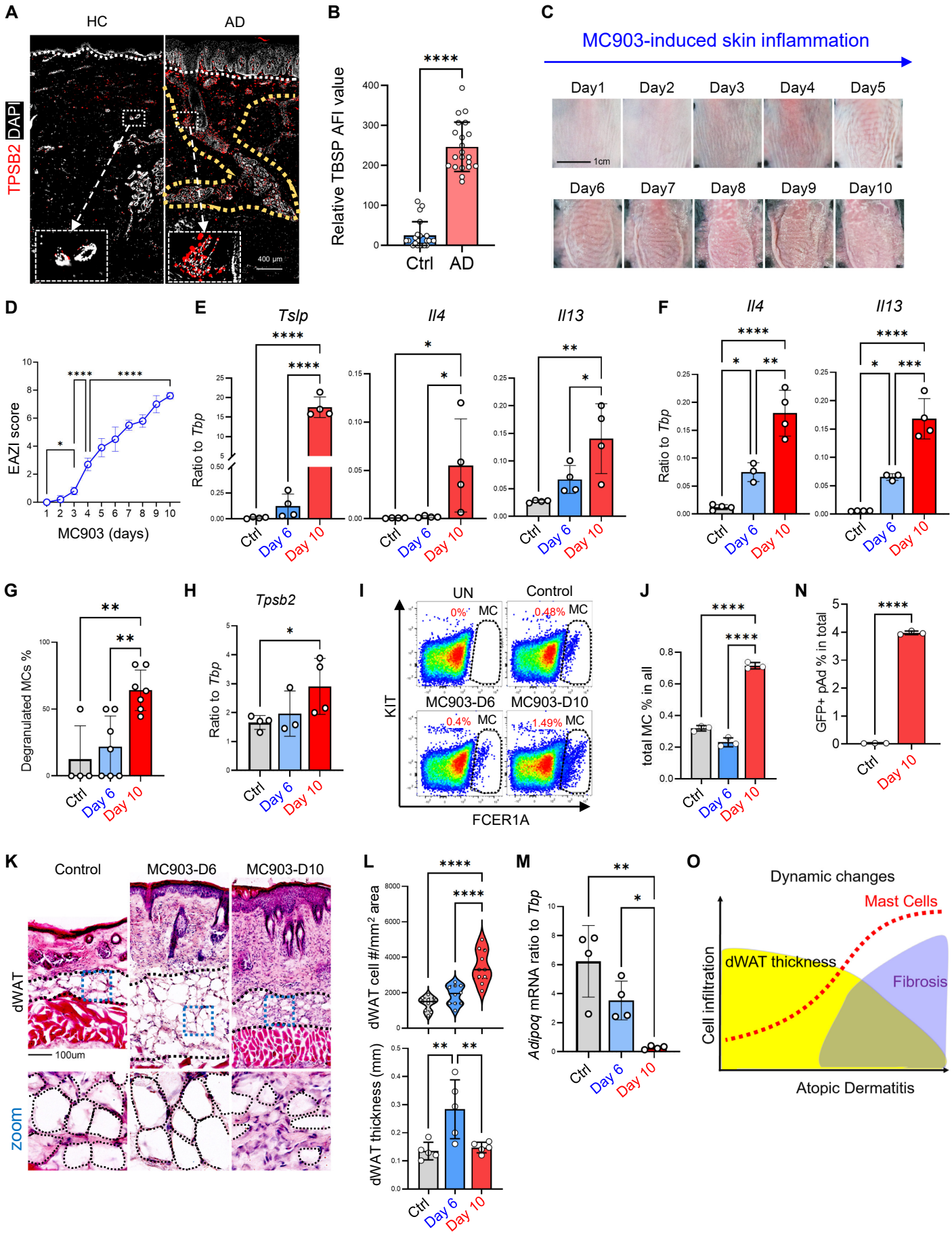
A
HC
AD
TPSB2 DAPI
400 μm
B
Relative TBSP AFI value
****
Ctrl
AD
C
MC903-induced skin inflammation
Day1
Day2
Day3
Day4
Day5
1cm
Day6
Day7
Day8
Day9
Day10
D
EAZI score
MC903 (days)
E
Tslp
Il4
Il13
Ratio to Tbp
Ctrl
Day 6
Day 10
F
Il4
Il13
Ratio to Tbp
G
Degranulated MCs %
H
Tpsb2
Ratio to Tbp
I
UN
Control
0%
MC
0.48%
MC903-D6
MC903-D10
0.4%
1.49%
KIT
FCER1A
J
total MC % in all
N
GFP+ pAd % in total
K
Control
MC903-D6
MC903-D10
dWAT
100um
zoom
L
dWAT cell #/mm2 area
dWAT thickness (mm)
M
Adipoq mRNA ratio to Tbp
O
Dynamic changes
Mast Cells
dWAT thickness
Fibrosis
Cell infiltration
Atopic Dermatitis

FIGURE S1

FIGURE S1. Spatiotemporal coupling of adipocyte lipolysis and dedifferentiation to mast cell activation and fibrotic remodeling during AD pathogenesis

(**A**-**B**) Formalin-fixed, paraffin-embedded human biopsies (healthy control/HC and atopic dermatitis lesional) were sectioned and immunostained for TPSB2 (red) and DAPI (white) as indicated. White dotted-lines mark the boarder between the dermis and epidermis and yellow dotted-lines mark the fibrotic area enriched with $TPSB2^+$ mast cells and collagen bundles (see Fig. 1C). Scale bars, 400 μm. (**B**) Quantified results showing relative TPSB AFI (artificial fluorescent intensity) (n=~20 areas/group).

(**C-D**) Mouse back skin were applied topically with MC903 everyday for upto 10 days to induced AD-like skin inflammation. Macroscopic images (**C**) and quantified Atopic Dermatitis Severity Index (EASI) scores (**D**) showing the development of skin lesions overtime.
(**E**) qRT-PCR analysis of the mRNA expression of *Tslp, Il4, Il13* in mouse skin (n=4/group).

(**F**) qRT-PCR analysis of the mRNA expression of *Il4, Il13* in skin-draining lymph nodes (n=4/group).

(**G**) Quantified bar graph showing the percentage of degranulated mast cells (Fig. 1F) in dWAT.

(**H**) qRT-PCR analysis of the mRNA expression of *Tpsb2* in mouse skin (n=4/group).

(**I-J**) FACS plots (**I**) showing the percentage of mast cells ($KIT^+FCER1A^+$) in total skin cells isolated from control or MC903-treated skin samples as indicated (representative of n= 3/group). (**J**) Quantified bar graphs showing the percentage of $KIT^+FCER1A^+$ mast cells in total cells (n = 3/group).

(**K-L**) Representative Hematoxylin-Erosin (H&E) staining of control or MC903-treated mouse skin samples. Zoom-in images of dWAT are shown on the lower panel. (**L**) Quantified bar graphs showing dWAT cell #/mm^2 area or dWAT thickness as indicated (n=8~9/group).
(**M**) qRT-PCR analysis of the mRNA expression of *Adipoq* in mouse skin (n=4/group).

(**N**) Adipoq-CreERT2;mTmG mice were injected with tamoxifen, treated with MC903 and dorsal skin was analyzed by FACS analysis as shown in Fig. 1P. Quantified bar graphs showing the percentage of GFP^+ $PDGFRA^+$ $Ly6A^+$ preadipocytes (pAds) in total cells (n = 3/group).

(**O**) Proposed model depicting the temporal evolution of MC903-induced AD-like inflammation: dWAT thickness rapidly declines (lipolysis), mast-cell infiltration and activation rises, followed by progressive accumulation of dermal collagen (fibrosis).

All error bars indicate mean ± SEM. *p < 0.05, **p < 0.01, ***p < 0.001, ****p < 0.0001.

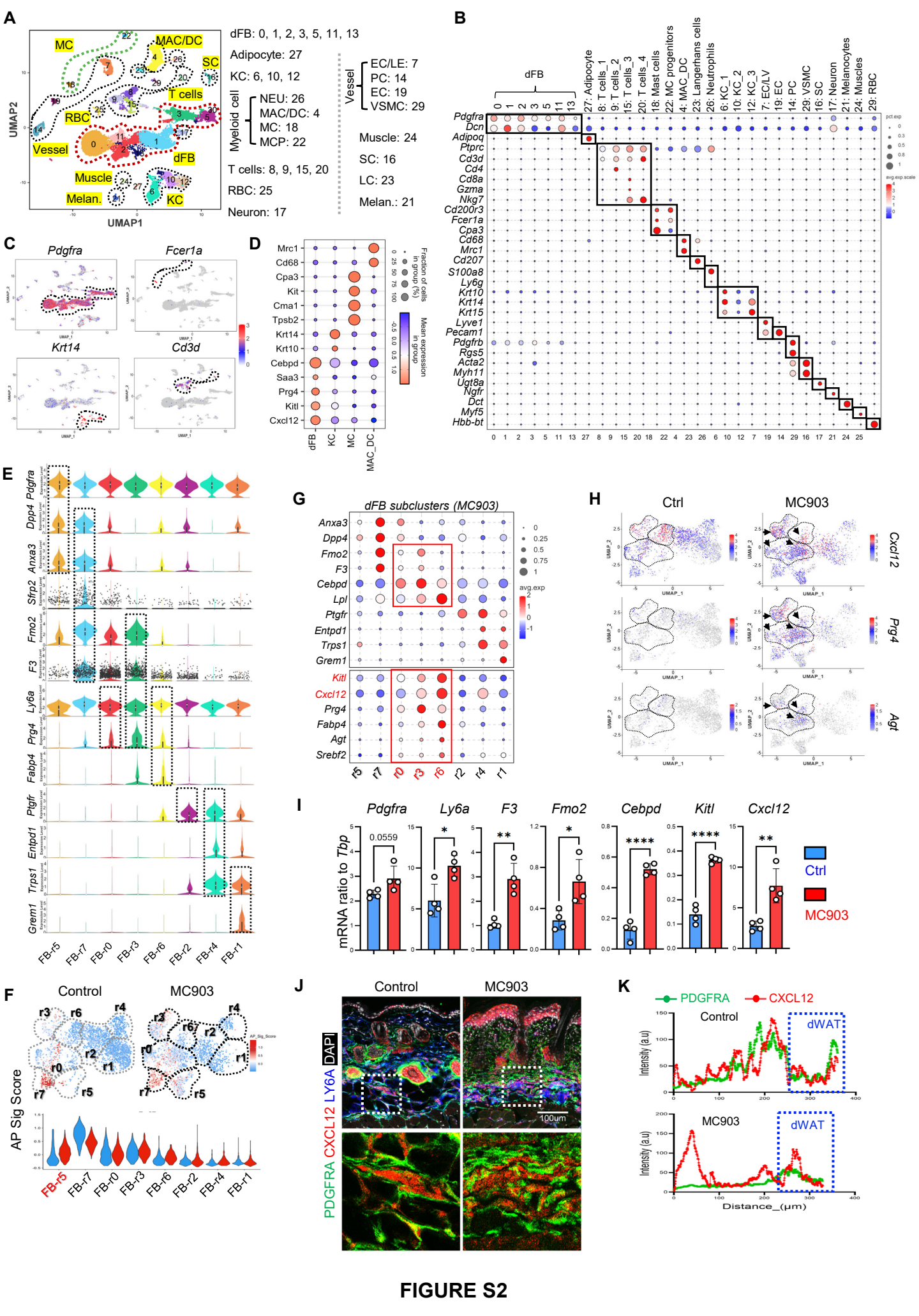
A
MC
MAC/DC
SC
T cells
RBC
Vessel
dFB
Muscle
Melan.
KC
UMAP1
UMAP2
dFB: 0, 1, 2, 3, 5, 11, 13
Adipocyte: 27
KC: 6, 10, 12
Myeloid cell
NEU: 26
MAC/DC: 4
MC: 18
MCP: 22
Vessel
EC/LE: 7
PC: 14
EC: 19
VSMC: 29
T cells: 8, 9, 15, 20
Muscle: 24
SC: 16
RBC: 25
LC: 23
Neuron: 17
Melan.: 21
B
dFB
0 1 2 3 5 11 13
27: Adipocyte
8: T cells_1
9: T cells_2
15: T cells_3
20: T cells_4
18: Mast cells
22: MC progenitors
4: MAC_DC
23: Langerhans cells
26: Neutrophils
6: KC_1
10: KC_2
12: KC_3
7: EC/LV
19: EC
14: PC
29: VSMC
16: SC
17: Neuron
21: Melanocytes
24: Muscles
29: RBC
Pdgfra
Dcn
Adipoq
Ptprc
Cd3d
Cd4
Cd8a
Gzma
Nkg7
Cd200r3
Fcer1a
Cpa3
Cd68
Mrc1
Cd207
S100a8
Ly6g
Krt10
Krt14
Krt15
Lyve1
Pecam1
Pdgfrb
Rgs5
Acta2
Myh11
Ugt8a
Ngfr
Dct
Myf5
Hbb-bt
0 1 2 3 5 11 13 27 8 9 15 20 18 22 4 23 26 6 10 12 7 19 14 29 16 17 21 24 25
C
Pdgfra
Fcer1a
Krt14
Cd3d
D
Mrc1
Cd68
Cpa3
Kit
Cma1
Tpsb2
Krt14
Krt10
Cebpd
Saa3
Prg4
Kitl
Cxcl12
dFB
KC
MC
MAC_DC
Fraction of cells in group (%)
Mean expression in group
E
Pdgfra
Dpp4
Anxa3
Sfrp2
Fmo2
F3
Ly6a
Prg4
Fabp4
Ptgfr
Entpd1
Trps1
Grem1
FB-r5
FB-r7
FB-r0
FB-r3
FB-r6
FB-r2
FB-r4
FB-r1
G
dFB subclusters (MC903)
Anxa3
Dpp4
Fmo2
F3
Cebpd
Lpl
Ptgfr
Entpd1
Trps1
Grem1
Kitl
Cxcl12
Prg4
Fabp4
Agt
Srebf2
r5 r7 r0 r3 r6 r2 r4 r1
avg.exp
H
Ctrl
MC903
Cxcl12
Prg4
Agt
I
Pdgfra
Ly6a
F3
Fmo2
Cebpd
Kitl
Cxcl12
mRNA ratio to Tbp
0.0559
*
**
*
****
****
**
Ctrl
MC903
F
Control
MC903
r0
r1
r2
r3
r4
r5
r6
r7
AP Sig Score
FB-r5
FB-r7
FB-r0
FB-r3
FB-r6
FB-r2
FB-r4
FB-r1
J
Control
MC903
DAPI
PDGFRA CXCL12 LY6A
100um
K
PDGFRA
CXCL12
Control
dWAT
MC903
dWAT
Intensity (a.u)
Distance_(μm)

FIGURE S2

FIGURE S2. Defining the dermal immune landscape of Pdgfra$^+$ fibroblast subsets by scRNA-seq
(**A-D**) ScRNA-seq analysis of total skin cells from Ctrl and MC903-induced mice. (**A**) UMAP projection of all skin cells, showing cell distribution by clusters. The identify for each cell cluster is shown on the right panel. Abbreviations: dFB, dermal fibroblasts; KC, keratinocytes; NEU, neutrophils; MAC, macrophages; MC, mast cells; MCP, mast cell progenitors; RBC, red blood cells; EC, endothelial cells; LV, lymphatic vessel; VSMC, vascular smooth muscle cells; SC, Schwann cells; Melan, melanocytes. (**B**) Bubble plots showing marker gene expression for each cell cluster. (**C**) UMAP plots showing the expression of *Pdgfra* (dFB marker), *Krt14* (KC marker), *Fcer1a* (MC marker), and *Cd3d* (T cell marker). (**D**) Bubble plots showing the differentially expressed genes in dFBs, KC, MC, and MAC_DC cell populations.

(**E-H**) PDGFRA$^+$ dFBs were re-clustered into 8 sub-clusters as shown in Fig. 2D-E. (**E**) Violin plots showing the expression of indicated marker genes for each dFB cluster. (**F**) Signature score distribution shown on UMAP and violin plots for adipocyte progenitor (AP) gene signature. (**G**) Bubble plots showing the differential expressed genes in various *Pdgfra*$^+$ dFB clusters in MC903-treated skin samples. (**H**) UMAP plots showing the expression of indicated genes in control and MC903 skin samples.

(**I**) qRT-PCR analysis of indicated genes in control or MC903-treated skin samples (n=4/group). All error bars indicate mean $\pm$ SEM. *p < 0.05, **p < 0.01, ****p < 0.0001.

(**J-K**) Immunostaining of CXCL12 (red), Ly6A (blue), PDGFRA (green) and DAPI (white) in control or MC903-treated skin samples. Scale bar, 100 μm. Quantified fluorescence intensity profiles of PDGFRA (green) and CXCL12 (red) measured from the epidermis through dWAT.

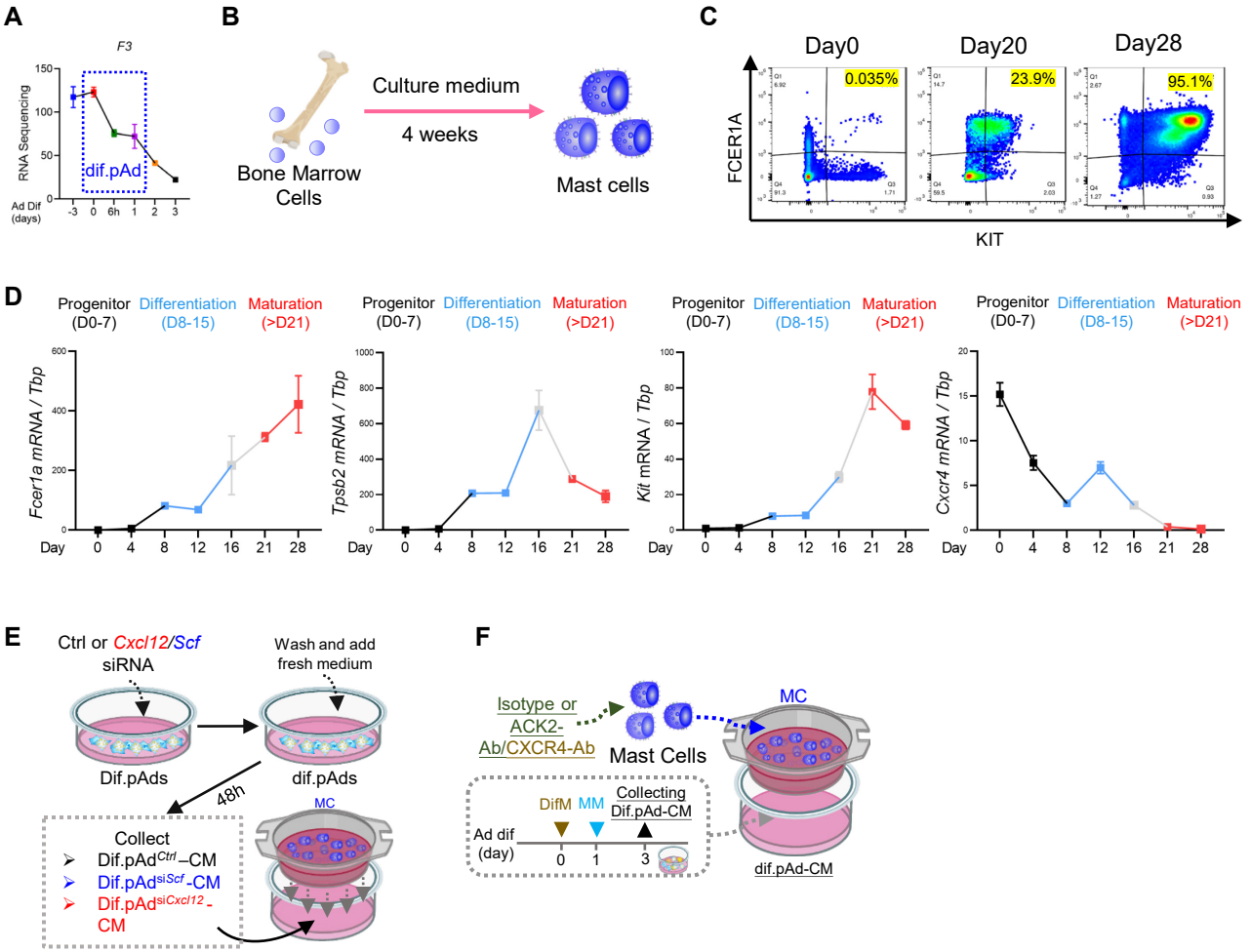

FIGURE S3. Inflammatory pAds are the dominant cellular source of the MC chemoattractants SCF and CXCL12 in AD skin.

(**A**) Line chart showing the mRNA expression kinetics of *F3* during in vitro adipocyte differentiation course.

(**B-D**) Schematic diagram **(B)** for in vitro mast cell culture and FACS plot showing the percentage of mast cells (KIT+FCER1A+) in total viable cells **(C)**. **(D)** qRT-PCR analysis of mRNA expression levels of indicated genes during in vitro mast cell culture.

(**E**) Schematic diagram showing the strategy to establish the co-culture system between bone-marrow derived MCs and dif. pAd transfected with dsiRNA against Scf or Cxcl12 in a transwell system.

(**F**) Schematic diagram showing the strategy to establish thetranswell system between dif. pAd-CM and bone-marrow derived MCs pretreated with neutralizing antibody against ACK2 or CXCR4 neutralizing antibody.

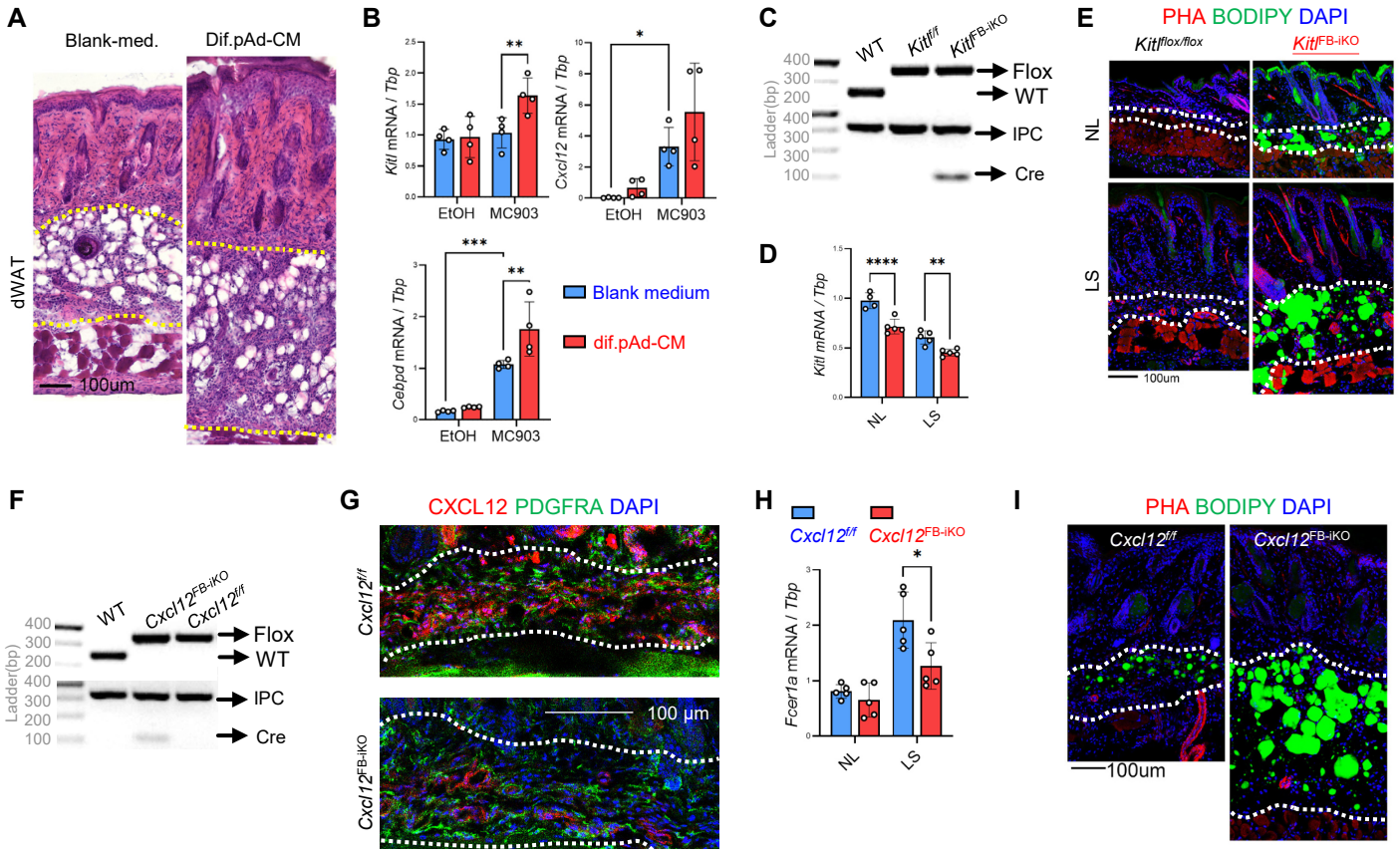

FIGURE S4. Fibroblast-specific ablation of *Kitl* or *Cxcl12* abolishes mast cell influx and fibrosis in dWAT during AD pathogenesis

(**A-B**) Mice undergoing daily MC903 treatment received intradermal injections of control or dif. pAd_CM as indicated in Fig. 4A, and skin samples were collected at day 6 of treatment for analysis. (**A**) Representative HE staining images. (**B**) qRT-PCR analysis of indicated genes (n=4/group).

(**C-E**) The inducible fibroblast-specific *Kitl* mice (*Kitl* $^{f/f}$;*Pdgfra-Cre*/ERT, *Kitl* $^{FB\text{-}iKO}$) were injected i.p. with TAM during the MC903 application course. (**C**) Multiplex-PCR based genotyping using allele specific primers yields DNA products having sizes specific for the wild-type and *Kitl*-floxed alleles. Lower gel shows gene products for Cre and/or internal product control (IPC) as indicated. (**D**) qRT-PCR analysis of *Kitl* (n=5/group). (**E**) Skin sections were stained with bodipy (green), PHA (red), and DAPI (blue). The dotted lines mark dWAT layer. Scale bars, 100 um.

(**F-I**) The inducible fibroblast-specific *Cxcl12* mice (Cxcl12$^{f/f}$;*Pdgfra-Cre*/ERT, *Cxcl12*$^{FB\text{-}iKO}$) were injected i.p. with TAM during the MC903 application course. (**F**) Multiplex-PCR based genotyping using allele specific primers yields DNA products having sizes specific for the wild-type and *Cxcl12*-floxed alleles. Lower gel shows gene products for Cre and/or internal product control (IPC) as indicated. (**G**) qRT-PCR analysis of *Fcer1a* (n=5/group). (**H**) Immunostaining of CXCL12 (red), PDGFRA (blue), and DAPI (white). The dotted lines mark dWAT layer. Scale bars, 100 um. (**I**) Skin sections were stained with bodipy (green), PHA (red), and DAPI (blue). The dotted lines mark dWAT layer. Scale bars, 100 um.

All error bars indicate mean ± SEM. *p < 0.05, **p < 0.01, ***p < 0.001, ****p < 0.0001.

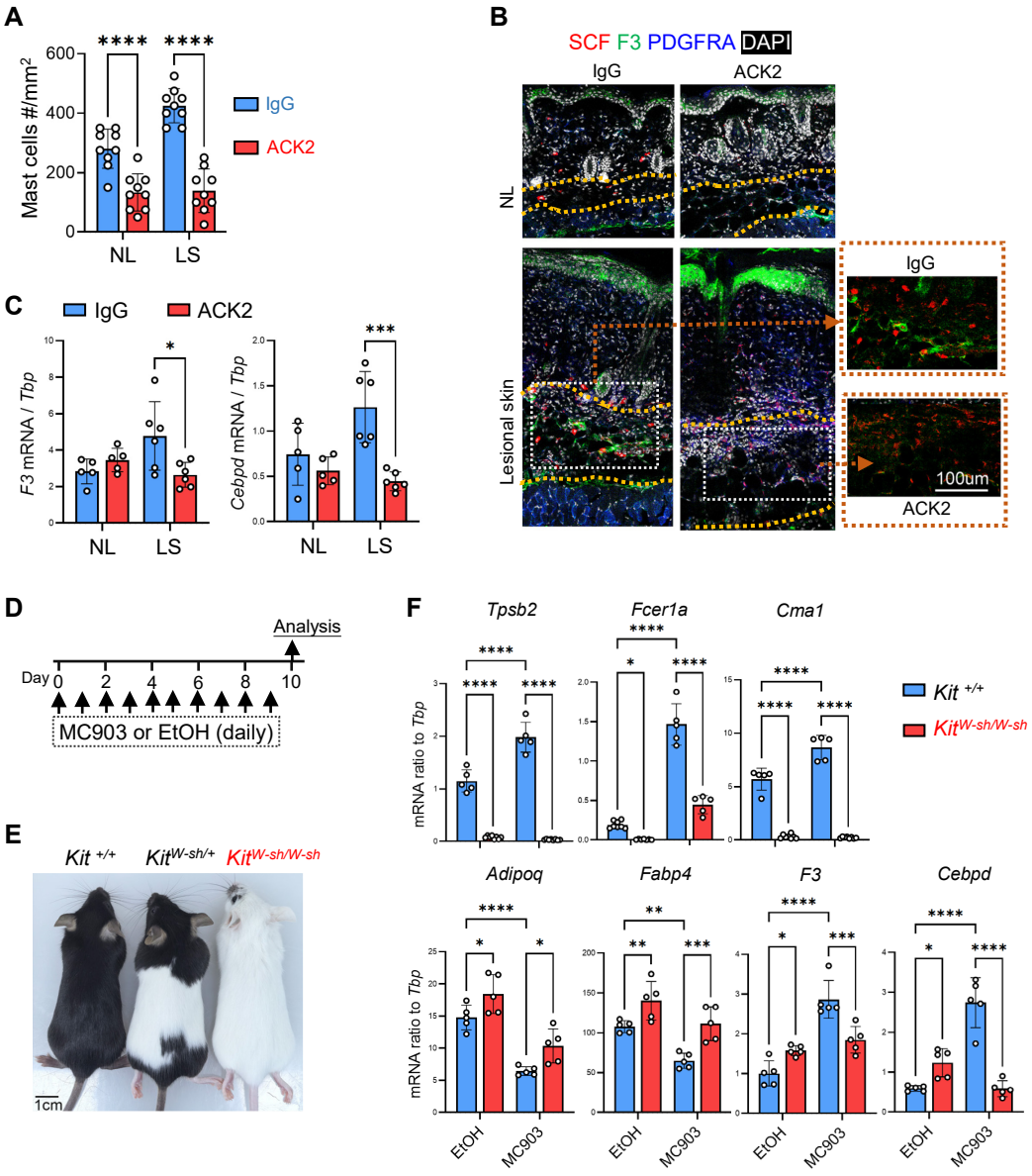

FIGURE S5. Mast cells are required for adipocyte lipolysis, pAd activation, and dWAT fibrosis in AD

(**A-C**) Anti-ACK2 antibody or rat IgG2A isotype control antibody was injected intradermal during MC903-application, and skin biopsies were collected for analysis. (**A**) Quantified bar graphs of Fig. 5D showing the number of MCs/mm^2 (n=9/group). (**B**) Immunostaining of SCF (red), F3 (green), PDGFRA (blue), and DAPI (white). The dotted lines mark dWAT layer. Zoom-in panels for red and green fluorescence channels are shown on the right panels. Scale bars, 100 um. (**C**) qRT-PCR analysis of the listed genes in EtOH or MC903-treated skin samples (n=5-6/group).

(**D-F**) Wild type (WT) and *Kit* $^{W\text{-}sh/W\text{-}sh}$ mice were subjected to daily MC903 applications for 10 days (schematic in **D**). (**E**) Representative mouse back skin images for each genotype. **(F)** qRT-PCR analysis of the listed genes in EtOH or MC903-treated skin samples (n=5/group).

All error bars indicate mean ± SEM. *p < 0.05, **p < 0.01, ***p < 0.001, ****p < 0.0001.

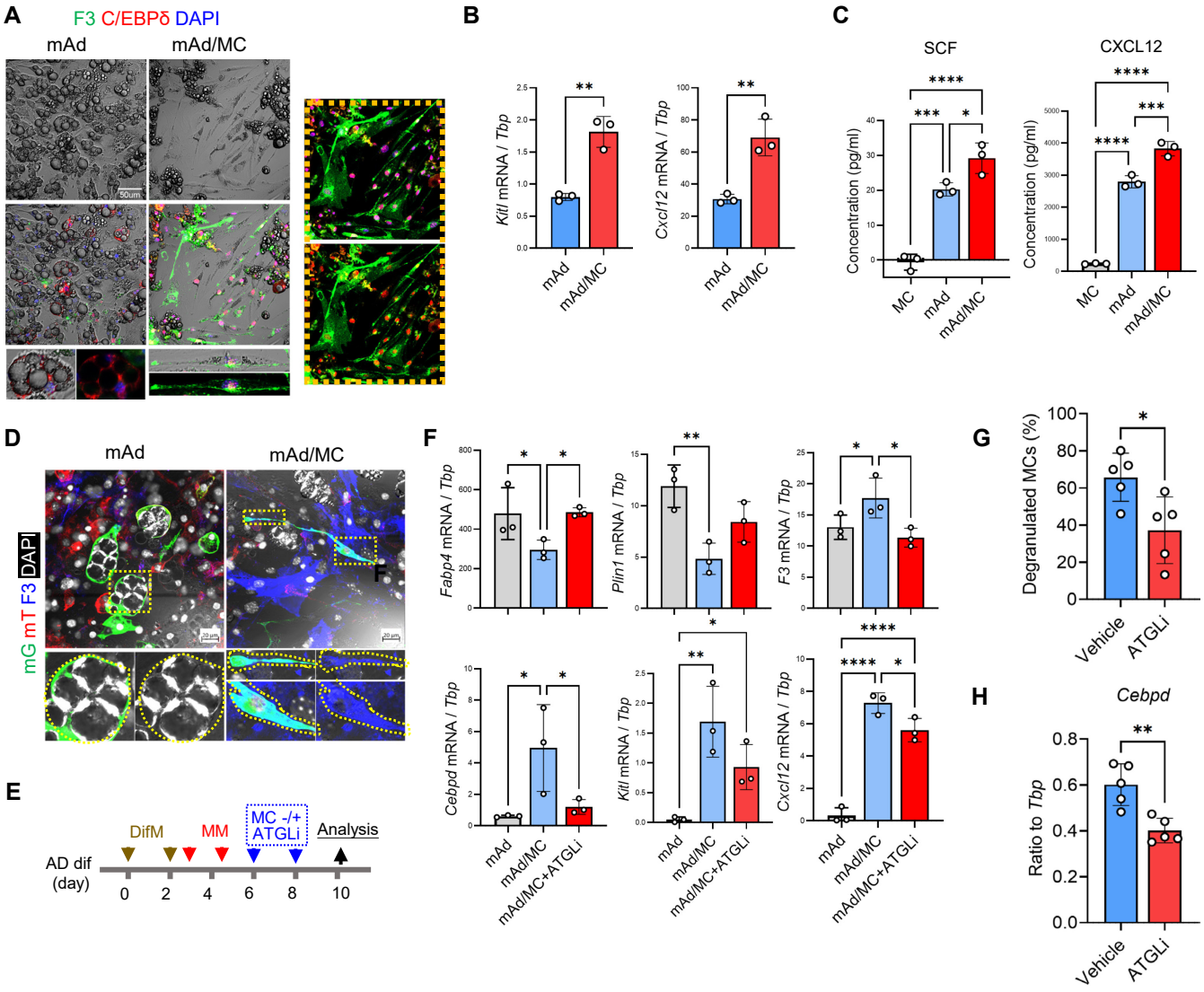

FIGURE S6. Mast cells trigger lipolysis-dependent adipocyte-to-inflammatory pAds trans-differentiation

(**A-C**) Fully differentiated adipocytes were cocultured with MC as shown in Fig. 6A. (**A**) Overlaid wild-filed image and immunostaining image of F3 (green), C/EBPδ (red), DAPI (blue). Scale bars ,50 μm. (**B**) qRT-PCR analysis of the indicated genes (n = 3/group). (**C**) ELISA analysis measuring the secreted protein concentration of SCF and CXCL12 (n=3/group).

(**D**) Primary neonatal dFBs isolated from Adipoq-CreERT2;mTmG mice were differentiated into mature adipocytes in the presence of TAM and then cocultured with MCs. Immunostaining with F3 antibody (blue) and DAPI (white). Scale bars, 20 μm.

(**E-F**) ATGL inhibitor-pretreated mature adipocytes were co-cultured with MCs (schematic diagram in **E**). (**F**) qRT-PCR analysis of the indicated genes (n = 3/group).

(**G-H**) Mice were i.p. injected daily with ATGLi or vehicle during MC903 applications. (**G**) Quantified the results of Fig. 6K showing the number of degranulating MCs/mm^2 in dWAT (n=5/group). (**H**) qRT-PCR analysis of *Cebpd* (n = 5/group).有5个点

All error bars indicate mean ± SEM. *p < 0.05, **p < 0.01, ***p < 0.001, ****p < 0.0001.

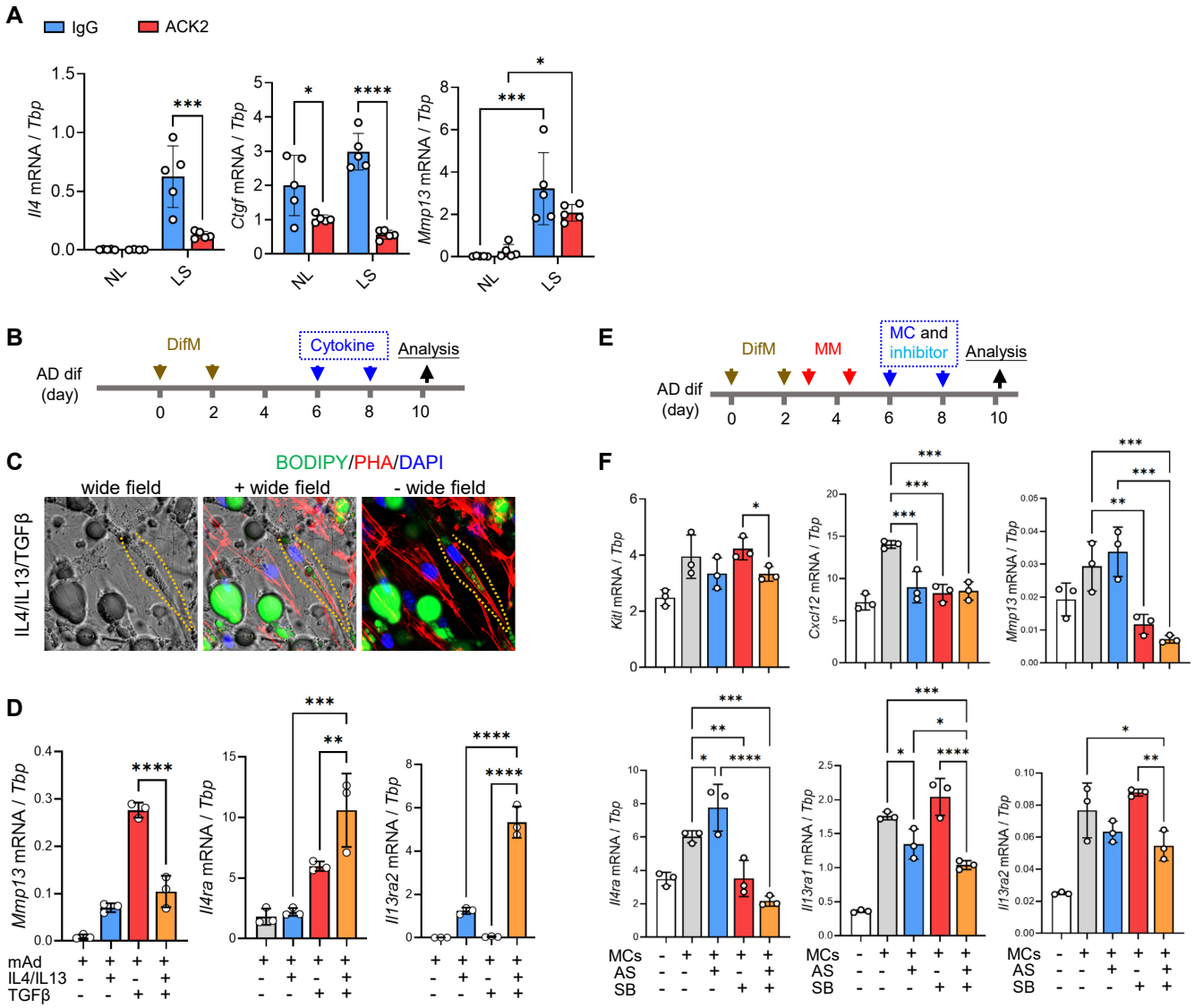

FIGURE S7. Mast Cells Induce dWAT Fibrosis via IL-4/IL-13/TGF-β Signaling

(**A**) Anti-KIT antibody or rat IgG2A isotype control antibody was injected intradermal to mouse skin during MC903-application, and skin biopsies were collected for qRT-PCR analysis of indicated genes (n =3~5/group).

(**B-D**) Mature adipocytes were co-treated with IL4, IL13, and TGFβ for 4 days (schematic diagram in **B**). (**C**) Wide-field images are overlaid with BODIPY (green), PHA (red) and DAPI (blue) staining images. (**D**) qRT-PCR analysis of the indicated genes (n = 3/group).

(**E-F**) STAT6 and/or TGFBR inhibitor-pretreated fully differentiated adipocytes were co-cultured with MCs (schematic diagram in **E**). (**F**) qRT-PCR analysis of the indicated genes (n = 3/group).

All error bars indicate mean ± SEM. *p < 0.05, **p < 0.01, ***p < 0.001, ****p < 0.0001.

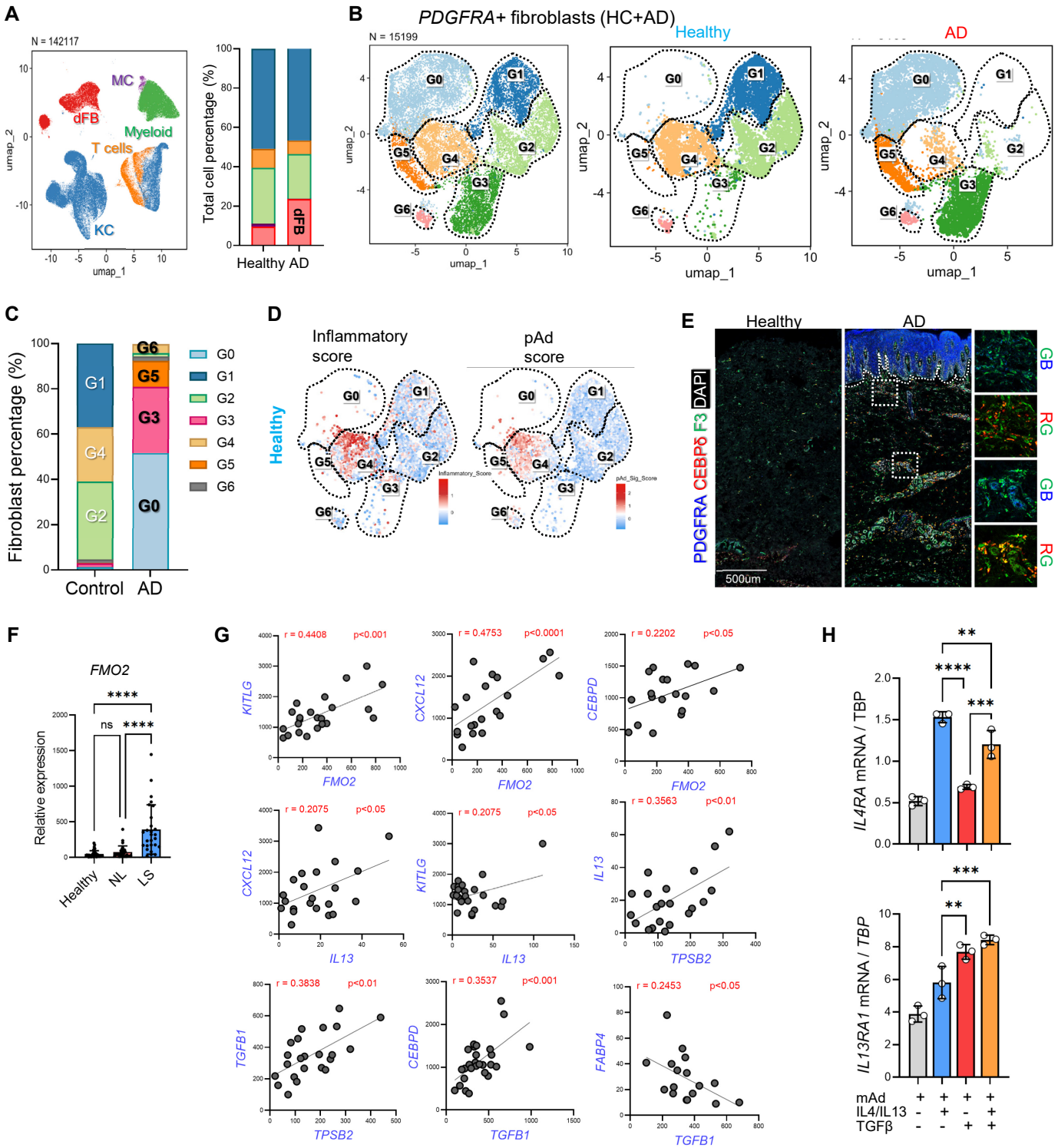
A
N = 142117
MC
dFB
Myeloid
T cells
KC
umap_1
umap_2
Total cell percentage (%)
Healthy AD
B
PDGFRA+ fibroblasts (HC+AD)
N = 15199
Healthy
AD
G0
G1
G2
G3
G4
G5
G6
C
Fibroblast percentage (%)
Control
AD
D
Inflammatory score
pAd score
Healthy
E
Healthy
AD
DAPI
PDGFRA CEBPδ F3
GB
RG
500um
F
FMO2
Relative expression
ns
****
Healthy
NL
LS
G
r = 0.4408 p<0.001
r = 0.4753 p<0.0001
r = 0.2202 p<0.05
r = 0.2075 p<0.05
r = 0.2075 p<0.05
r = 0.3563 p<0.01
r = 0.3838 p<0.01
r = 0.3537 p<0.001
r = 0.2453 p<0.05
KITLG
CXCL12
CEBPD
IL13
TPSB2
TGFB1
FABP4
H
IL4RA mRNA / TBP
IL13RA1 mRNA / TBP
mAd
IL4/IL13
TGFβ

FIGURE S8

FIGURE S8. Preadipocyte and Inflammatory Signature Define Inflammatory Fibroblasts in Human Atopic Dermatitis

(**A-D**) ScRNA-seq data of human psoriasis database (Reynolds et al., 2021). (**A**) UMAP plots (left) and bar graphs (right) showing cell distribution and percentage of dFB, KC, T cells, MC and myeloid cell populations in healthy and AD skin samples. (**B**) UMAP plots showing by clusters (left panel) or by samples (middle and right panels) distribution of 7 *PDGFRA*$^+$ dFB clusters (G0-G6) from HC and AD skin samples. (**C**) Bar graphs showing cell percentage of *PDGFRA*+ dFB. (**D**) UMAP showing the distribution of preadipocytes or inflammatory signature scores in human healthy skin.

(**E**) Immunostaining of C/EBPδ (red), F3 (green), PDGFRA (blue), and DAPI (blue) in skin sections from human healthy and AD skin samples. White dotted lines separate the epidermis from the dermis. Zoom-in panels for indicated RGB channels are shown on the right. Scale bar, 500 μm.

(**F**) Bar graphs showing the expression (based on RNAseq FPKM values) of *FMO2* in human healthy (healthy), non-lesional (NL) and lesional (LS) skin samples (n>30/group).

(**G**) Correlation expression plots of indicated genes. Linear correlation analysis was performed by Pearson correlation coefficient method. The r value represents the correlation coefficent strength, and p value assesses the statistic significance of the correlation.

(**H**) In vitro human adipocytes were co-treated with cytokines, including IL4, IL13, and TGFβ for 4 days. qRT-PCR analysis of the indicated genes (n = 3/group).

All error bars indicate mean ± SEM. n.s., non-significant, **p < 0.01, ***p < 0.001, ****p < 0.0001.

Table S1. List of Abbreviations:

Abbreviations	Definitions
AP	Adipocyte progenitor
Ad	Adipocyte
MC903	Calcipotriol
AD	Atopic Dermatitis
HC	Healthy control
dWAT	Dermal white adipose tissue
dFB	Dermal fibroblast
p.t	Post-treatment
KC	Keratinocyte
NEU	Neutrophil
MC	Mast cell
MAC	Macrophage
RET	Reticular
PAP	Papillary
Inf.pAd	Inflammatory preadipocyte
Areg	Adipose regulatory cell
AP	Adipocyte progenitor
pAd	Preadipocyte
eAd	Early adipocyte
mAd	Mature adipocyte
TIFF	TH2-interacting fascial fibroblasts
TAM	Tamoxifen
NL	Non-lesional
LS	Lesional skin
scRNA-seq	Single-cell RNA sequencing
UMAP	Uniform manifold approximation and projection
FACS	Fluorescence activated cell sorting
IHC	Immunohistochemistry
CM	Conditioned medium

Table S2 List of protein and gene symbols:

Proteins	**Protein symbols**	**Gene symbols**
Annexin A3	ANXA3	*Anxa3*
Adiponectin	ADIPOQ	*Adipoq*
Aggrecan core protein	PGCA	*Acan*
Arginase 1	ARG1	*Arg1*
CD3 antigen, epsilon polypeptide	CD3E	*Cd3e*
CD68, antigen	CD68	*Cd68*
Collagen	COL	*Col*
C-X-C motif chemokine	CXCL	*Cxcl*
C-X-C chemokine receptor	CXCR	*Cxcr*
CCAAT enhancer-binding protein delta	CEBPD	*Cebpd*
Cellular retinoic acid-binding protein 1	CRABP1	*Crabp1*
Dipeptidyl peptidase 4	DPP4	*Dpp4*
Ectonucleoside triphosphate diphosphohydrolase 1	ENTPD1	*Entpd1*
Fatty acid binding protein 4	FABP4	*Fabp4*
Fibronectin	FN1	*Fn1*
Dimethylaniline monooxygenase [N-oxide-forming] 2	FMO2	*Fmo2*
Coagulation factor III	CD142	*F3*
Gremlin 1	GREM1	*Grem1*
Haptoglobin	HPT	*Hp*
Stem cell factor	SCF	*Kitl*
Interleukin 3	IL3	*Il3*
Interleukin 4	IL4	*Il4*
Interleukin 13	IL13	*Il13*
Interleukin-4 receptor subunit alpha	IL4RA	*Il4ra*
Interleukin-13 receptor subunit alpha-1	IL13R1A	*Il13ra1*
Interleukin-13 receptor subunit alpha-2	IL13RA2	*Il13ra2*
Matrix metalloproteinase-13	MMP13	*Mmp13*
Keratin	KRT	*Krt*
Neutrophil gelatinase-associated lipocalin	NGAL	*Lcn2*
Lipoprotein lipase	LPL	*Lpl*
Lymphocyte antigen 6A-2/6E-1	LY6A	*Ly6a*
Lymphocyte antigen 6G	LY6G	*Ly6g*
Lymphatic vessel endothelial hyaluronan receptor	LYVE	*Lyve*
Lymphoid enhancer-binding factor 1	LEF1	*Lef1*
Lysozyme C-2	LYZ2	*Lyz2*
Leucine-rich repeat-containing G-protein coupled receptor 5	LGR5	*Lgr5*

Stromelysin 1	MMP3	*Mmp3*
Proliferation marker protein Ki-67	Ki67	*Mki67*
Peroxisome proliferator-activated receptor gamma	PPARG	*Pparg*
Perilipin	PLIN	*Plin*
Platelet-derived growth factor receptor alpha	PDGFRA	*Pdgfra*
Prostaglandin F2-alpha receptor	PF2R	*Ptgfr*
Protein tyrosine phosphatase receptor type C	CD45	*Ptprc*
Proteoglycan 4	PRG4	*Prg4*
Patatin-like phospholipase domain-containing protein 2	ATGL	*Pnpla2*
Platelet/endothelial cell adhesion molecule 1	CD31	*Pecam1*
Regulator of G-protein signaling 5	RGS5	*Rgs5*
Serum amyloid A3	SAA3	*Saa3*
Protein S100 A8	S10A8	*S100a8*
Sphingomyelin phosphodiesterase 3	NSMA2	*Smpd3*
secreted frizzled-related protein 2	SFRP2	*Sfrp2*
Transforming growth factor beta	TGFB	*Tgfb*
Zinc finger transcription factor Trps1	TRPS1	*Trps1*
Tenascin C	TNC	*Tnc*
vimentin	VIM	*Vim*
mRNA decay activator protein ZFP36	TTP	*Zfp36*
Tyrosine-protein kinase Kit	CD117	*Kit*
Tryptase beta-2	TPSB2	*Tpsb2*

Table S3. List of primers used for qRT-PCR of mouse genes: (related to experimental procedure “Quantitative reverse transcription-quantitative PCR (qRT-PCR) analyses”). Gene symbols and forward and reverse primer sequences for each gene are shown in the table below.

Gene name	Strand	Primer sequence
Tbp	Forward	CCTTGTACCCTTCACCAATGAC
	Reverse	ACAGCCAAGATTCACGGTAGA
Pdgfra	Forward	ATGAGAGTGAGATCGAAGGCA
	Reverse	CGGCAAGGTATGATGGCAGAG
Ly6a	Forward	GAGGCAGCAGTTATTGTGGAT
	Reverse	CGTTGACCTTAGTACCCAGGA
Pparg2	Forward	TCGCTGATGCACTGCCTATG
	Reverse	GAGAGGTCCACAGAGCTGATT
Adipoq	Forward	CACACCAGGCCGTGATGGCA
	Reverse	GAAGCCCCGTGGCCCTTCAG
Plin1	Forward	CTGTGTGCAATGCCTATGAGA
	Reverse	CTGGAGGGTATTGAAGAGCCG
Fabp4	Forward	GTGGGAGTGGGCTTTGCCACA
	Reverse	CACCAGGGCCCCGCCATCTA
Cd24a	Forward	TTCTGGCACTGCTCCTACC
	Reverse	GCGTTACTTGGATTTGGGGAA
Dpp4	Forward	TATGCCCAGTTTAACGACACAG
	Reverse	ACAGTTGGATTCACAGCTCCT
Cebpd	Forward	CAGCGCCTACATTGACTCCA
	Reverse	GTTGAAGAGGTCGGCGAAGA
F3	Forward	GCCATTTACAAACGCCCCAA
	Reverse	GCAGGGTGAGGAATGTACCA
Fmo2	Forward	CTGCCACTCAAGTCATTCCCA
	Reverse	GCCATCTTCAGAGATTCGACTCA
Cxcl12	Forward	TGCATCAGTGACGGTAAACCA
	Reverse	TTCTTCAGCCGTGCAACAATC
Tgfb1	Forward	GAGCCCGAAGCGGACTACTA
	Reverse	TGGTTTTCTCATAGATGGCGTTG
Il4	Forward	GTACCAGGAGCCATATCCACG
	Reverse	CACCTTGGAAGCCCTACAGAC
Il13	Forward	TGCTTGCCTTGGTGGTCTCGC
	Reverse	GCGGCCAGGTCCACACTCCA
Il4ra	Forward	TCTGCATCCCGTTGTTTTGC
	Reverse	GCACCTGTGCATCCTGAATG
Il13ra1	Forward	AGAAGCCTAGCCCTTTGGTG
	Reverse	GGGAGCCAGGAACACTTCAT
Il13ra2	Forward	TGGCAGTATTTGGTCTGCTCT

	Reverse	CAAGCCCTCATACCAGAAAAACA
Cxcr4	Forward	GACTGGCATAGTCGGCAATG
	Reverse	AGAAGGGGAGTGTGATGACAAA
Mmp13	Forward	CTATCCCTTGATGCCATTACCAG
	Reverse	ATCCACATGGTTGGGAAGTTC
Ctgf	Forward	GGGCCTCTTCTGCGATTTC
	Reverse	ATCCAGGCAAGTGCATTGGTA
Kitl	Forward	GAATCTCCGAAGAGGCCAGAA
	Reverse	GCTGCAACAGGGGGTAACAT
Tpsb2	Forward	CGGAGGTTCTCTCATCCATCC
	Reverse	GCCGTGTAATAGTGGGGGTG
cKit	Forward	GGCCTCACGAGTTCTATTTACG
	Reverse	GGGGAGAGATTTCCCATCACAC
Cma1	Forward	CACGGAGTGCATACCACACT
	Reverse	AAGCTTCTGCCACGTGTCTT
Tgfb	Forward	CAGTGGGAAGACCCCACATC
	Reverse	TGTAAAGAGGGCGAAGGCAG
Fcer1a	Forward	GAGTGCCACCGTTCAAGACA
	Reverse	GTAGATCACCTTGCGGACATTC

Table S4. List of primers used for qRT-PCR of human genes: (related to experimental procedure “Quantitative reverse transcription-quantitative PCR (qRT-PCR) analyses”). Gene symbols and forward and reverse primer sequences for each gene are shown in the table below.

Gene name	Strand	Primer sequence
TBP	Forward	CCCGAAACGCCGAATATAATCC
	Reverse	AATCAGTGCCGTGGTTCGTG
FABP4	Forward	ACTGGGCCAGGAATTTGACG
	Reverse	CTCGTGGAAGTGACGCCTT
CEBPD	Forward	CCATGTACGACGACGAGAGC
	Reverse	TTGCTGTTGAAGAGGTCGGC
F3	Forward	TCGCTGATGCACTGCCTATG
	Reverse	GAGAGGTCCACAGAGCTGATT
ADIPOQ	Forward	AGGAAACCACGACTCAAGGG
	Reverse	TCCGGTTTCACCGATGTCTC
KITLG	Forward	AATCCTCTCGTCAAAACTGAAGG
	Reverse	CCATCTCGCTTATCCAACAATGA
IL4RA	Forward	ACCTGCGTCTCCGACTACA
	Reverse	TTATCCGCACTGACCACGTC
IL13RA1	Forward	TGAGTGTCTCTGTTGAAAACCTC
	Reverse	GGGGTACTTCTATTGAACGACGA
IL13RA2	Forward	ACCTGGCATAGGTGTACTTCT
	Reverse	CCAAATAGGGAAATCTGCATCCT
CXCL12	Forward	ATTCTCAACACTCCAAACTGTGC
	Reverse	ACTTTAGCTTCGGGTCAATGC
PPARG	Forward	ACCAAAGTGCAATCAAAGTGGA
	Reverse	ATGAGGGAGTTGGAAGGCTCT